CORE
Metadata, citation and similar papers at core.ac.uk
Provided by Elsevier - Publisher Connector

Neuron, Vol. 16, 333–344, February, 1996, Copyright ©1996 by Cell Press

Impairment of Suckling Response, Trigeminal Neuronal Pattern Formation, and Hippocampal LTD in NMDA Receptor ε2 Subunit Mutant Mice

Tatsuya Kutsuwada,[1,2]* Kenji Sakimura,[1]* Toshiya Manabe,[3] Chitoshi Takayama,[4] Nobuo Katakura,[5] Etsuko Kushiya,[1] Rie Natsume,[1] Masahiko Watanabe,[4] Yoshiro Inoue,[4] Takeshi Yagi,[6]† Shinichi Aizawa,[6]‡ Masaaki Arakawa,[2] Tomoyuki Takahashi,[3] Yoshio Nakamura,[5] Hisashi Mori,[7] and Masayoshi Mishina[1,7]

[1]Department of Neuropharmacology
Brain Research Institute
[2]Department of Internal Medicine II
Faculty of Medicine
Niigata University
Niigata 951
Japan
[3]Department of Neurophysiology
Institute for Brain Research
Faculty of Medicine
University of Tokyo
Tokyo 113
Japan
[4]Department of Anatomy
Hokkaido University School of Medicine
Sapporo 060
Japan
[5]Department of Physiology
Faculty of Dentistry
Tokyo Medical and Dental University
Tokyo 113
Japan
[6]Laboratory of Molecular Oncology
Tsukuba Life Science Center
Institute of Physical and Chemical Research
Ibaraki 305
Japan
[7]Department of Pharmacology
Faculty of Medicine
University of Tokyo
Tokyo 113
Japan

Summary

Multiple ε subunits are major determinants of the NMDA receptor channel diversity. Based on their functional properties in vitro and distributions, we have proposed that the ε1 and ε2 subunits play a role in synaptic plasticity. To investigate the physiological significance of the NMDA receptor channel diversity, we generated mutant mice defective in the ε2 subunit. These mice showed no suckling response and died shortly after birth but could survive by hand feeding. The mutation hindered the formation of the whisker-related neuronal barrelette structure and the clustering of primary sensory afferent terminals in the brainstem trigeminal nucleus. In the hippocampus of the mutant mice, synaptic NMDA responses and long-term depression were abolished. These results suggest that the ε2 subunit plays an essential role in both neuronal pattern formation and synaptic plasticity.

*These authors contributed equally to this work.
†Present address: Laboratory of Neurobiology and Behavioral Genetics, National Institute for Physiological Sciences, Okazaki 444, Japan.
‡Present address: Laboratory of Morphogenesis, Institute of Molecular Embryology and Genetics, Kumamoto University School of Medicine, Kumamoto 860, Japan.

Introduction

The N-methyl-D-aspartate (NMDA) receptor channel is unique in functional properties among many neurotransmitter receptors and ion channels mediating neural signaling in the brain. The NMDA receptor channel is gated by both ligands and voltage, and is highly permeable to Ca^{2+} (Mayer et al., 1984; Nowak et al., 1984; Ascher and Nowak, 1986; MacDermott et al., 1986). These characteristics of the NMDA receptor channel directly relate to its important physiological roles in synaptic plasticity as a molecular coincidence detector. Some forms of long-term potentiation (LTP) and long-term depression (LTD), which are thought to underlie learning and memory, are critically dependent on the NMDA receptor channel (Bliss and Collingridge, 1993; Malenka and Nicoll, 1993). The NMDA receptor channel is also involved in neuronal pattern formation during development (Cline et al., 1987; Kleinschmidt et al., 1987).

One of the most important findings obtained by recent molecular cloning is the elucidation of the molecular diversity of the NMDA receptor channel (Ikeda et al., 1992; Kutsuwada et al., 1992; Meguro et al., 1992; Monyer et al., 1992). Highly active NMDA receptor channel is formed in vitro by coexpression of two members of glutamate receptor (GluR) channel subunit families, i.e., the GluRε (the fifth subfamily or NR2) and GluRζ (the sixth subfamily or NR1) subunit families (Ikeda et al., 1992; Kutsuwada et al., 1992; Meguro et al., 1992; Monyer et al., 1992), although the ζ1 (NMDAR1) subunit alone exhibits a very small response at least in the Xenopus oocyte expression system (Moriyoshi et al., 1991; Yamazaki et al., 1992). In accord with this, most brain regions express both the ε and ζ subunit mRNAs, and no NMDA responses have been reported for maturated cerebellar Purkinje cells that express the ζ1 subunit but none of the ε subunits (Quinlan and Davies, 1985; Perkel et al., 1990; Watanabe et al., 1992, 1994a; Brose et al., 1993; Monyer et al., 1994). There are four members in the ε subunit family (Ikeda et al., 1992; Kutsuwada et al., 1992; Meguro et al., 1992; Monyer et al., 1992), whereas only one member is known in the ζ subunit family, except for the splice variants (Moriyoshi et al., 1991; Yamazaki et al., 1992). At the embryonic stages, the ε2 (NR2B) subunit mRNA is expressed in the entire brain, and the ε4 (NR2D) subunit mRNA in the diencephalon and the brainstem (Watanabe et al., 1992). After birth, the ε1 (NR2A) subunit mRNA appears in the entire brain, and the ε3 (NR2C) subunit mRNA mainly in the cerebellum. Expression of the ε2 subunit mRNA becomes restricted to the forebrain, and that of the ε4

subunit mRNA is strongly reduced. The ζ1 subunit mRNA is found ubiquitously in the brain during development. The four ε subunits are also distinct in functional properties and regulation (Mishina et al., 1993; Seeburg, 1993; Mori and Mishina, 1995). Thus, multiple ε subunits are major determinants of the NMDA receptor channel diversity, and the molecular compositions and functional properties of NMDA receptor channels are different depending on the brain regions and developmental stages. These findings raise an important question as to whether the molecular diversity underlies the various physiological roles of the NMDA receptor channel, or whether the same or different NMDA receptors are involved in synaptic plasticity and neuronal pattern formation during development, although various experiments with selective antagonists showed the physiological importance of the NMDA receptor channel (Bliss and Collingridge, 1993; Goodman and Shatz, 1993). Mutant mice defective in the common ζ1 subunit died shortly after birth and failed to develop whisker-related neuronal patterns in the trigeminal nuclei (Forrest et al., 1994; Li et al., 1994). Based on the higher sensitivity to Mg^{2+} block and strong expression in the hippocampus and cerebral cortex, we have proposed that the ε1 and ε2 subunits play a role in synaptic plasticity (Kutsuwada et al., 1992; Mishina et al., 1993).

To test our working hypothesis and to examine the functional roles in vivo of the diverse ε subunits of the NMDA receptor channel, we employed the gene targeting technique (Capecchi, 1989). We have shown that disruption of the ε1 subunit of the mouse NMDA receptor channel does not appreciably affect the growth and mating of the mice, but results in reduction of hippocampal LTP and spatial learning (Sakimura et al., 1995). The ε4 subunit mutant mice grow normally and develop whisker-related neuronal patterns in the trigeminal nuclei, but exhibit reduced spontaneous behavioral activity (Ikeda et al., 1995). In the present investigation, we report the characterization of mice defective in the ε2 subunit. The mutant mice died within 1 day after birth. However, we could rear the mice by hand feeding, making it possible to examine the effect of the disruption of the ε2 subunit gene on synaptic plasticity and neuronal pattern formation.

Results

Neonatal Death of Mice Defective in the ε2 Subunit of the NMDA Receptor Channel

To disrupt the GluRε2 locus in murine embryonic stem cells by homologous recombination, we constructed a targeting vector containing a 9.8 kb GluRε2 genomic DNA fragment in which the exon including the translation initiation site was interrupted by the insertion of the neomycin phosphotransferase gene (Figure 1A). Three clones with the disrupted GluRε2 gene were obtained by transfection of TT2 embryonic stem cells with the targeting vector, and chimeras derived from clones P60 and T43 transmitted the mutation through the germline. Heterozygous progenies were intercrossed, and the offspring were genotyped by Southern blot hybridization (Figure 1B). No homozygous mutant mice were found in 166 offspring of 5–6 weeks old. Among 77 newborn pups, however, there were 20 wild-type (+/+), 36 heterozygous (+/−), and 21 homozygous (−/−) mice, the ratio being close to 1:2:1.

Monitoring of newborn mice by a video camera showed that mothers delivered pups and nursed them normally. All newborn pups were reddish and appeared normal, suggesting that the cardiovascular and respiratory systems were functioning at birth. There was no significant difference in the average body weight among the wild-type (1.29 ± 0.03 g, mean ± SD; n = 19), heterozygous (1.27 ± 0.02 g; n = 30), and homozygous mutant (1.22 ± 0.02 g; n = 18) mice. Homozygous pups, however, had no milk in their stomachs even at 6–7 hr after birth, in contrast to their wild-type and heterozygous littermates, and could not survive for more than 1 day. Thus, the ε2 subunit gene is indispensable for mice.

We examined the expression of the NMDA receptor channel subunits by in situ hybridization analyses of parasagittal brain sections of newborn mice at postnatal day 0 (P0) with oligonucleotide probes (Figure 1C). The intact ε2 subunit mRNA was absent in the mutant mice as revealed by probe ε2C (corresponding to the disrupted region), while transcripts from the disrupted GluRε2 gene were detected by probe ε2A (corresponding to the intact region). Expression of the other NMDA receptor channel subunit mRNAs was not appreciably affected by the GluRε2 mutation. The ε4 subunit mRNA was mainly detected in the diencephalon and the brainstem, and the ζ1 subunit mRNA in the entire brain. The ε1 and ε3 subunit mRNAs were hardly detectable at P0, except for the ε1 subunit mRNA in the hippocampal CA1 region, as reported previously (Watanabe et al., 1992).

Western blot analysis of whole-brain proteins showed that homozygous mutant mice had no detectable GluRε2 protein (180 kDa), and the content of the protein of heterozygous mice was approximately half that of the wild-type mice (Figure 1D). The content of neuron-specific enolase (NSE), a marker protein of neurons (Schmechel et al., 1978), was not appreciably affected by the GluRε2 mutation.

Defect in Suckling Response

The suckling response includes the nipple attachment, suckling with rhythmic movements of the jaw and tongue, and the stretch response (Westneat and Hall, 1992). The rhythmic suckling movement can be induced by a mechanical stimulation of the lip. Most of the newborn mice showed a series of rhythmic jaw opening and closing movements in response to the tactile stimulation of the lip with a cannula. However, some pups failed to show this suckling behavior. Subsequent Southern blot analysis of their tail DNA indicated that the homozygous ε2 subunit mutant mice (n = 17) were defective in the suckling response, whereas the wild-type (n = 15) and heterozygous (n = 28) mice exhibited the response.

We also defined the suckling response by recording the movement of the tongue using electromyography (EMG). In response to a gentle touch with a soft cannula at the tip of the tongue, the wild-type mice showed a series of rhythmic suckling-like movements of the tongue (Figure 2, +/+). In contrast, the mutant mice

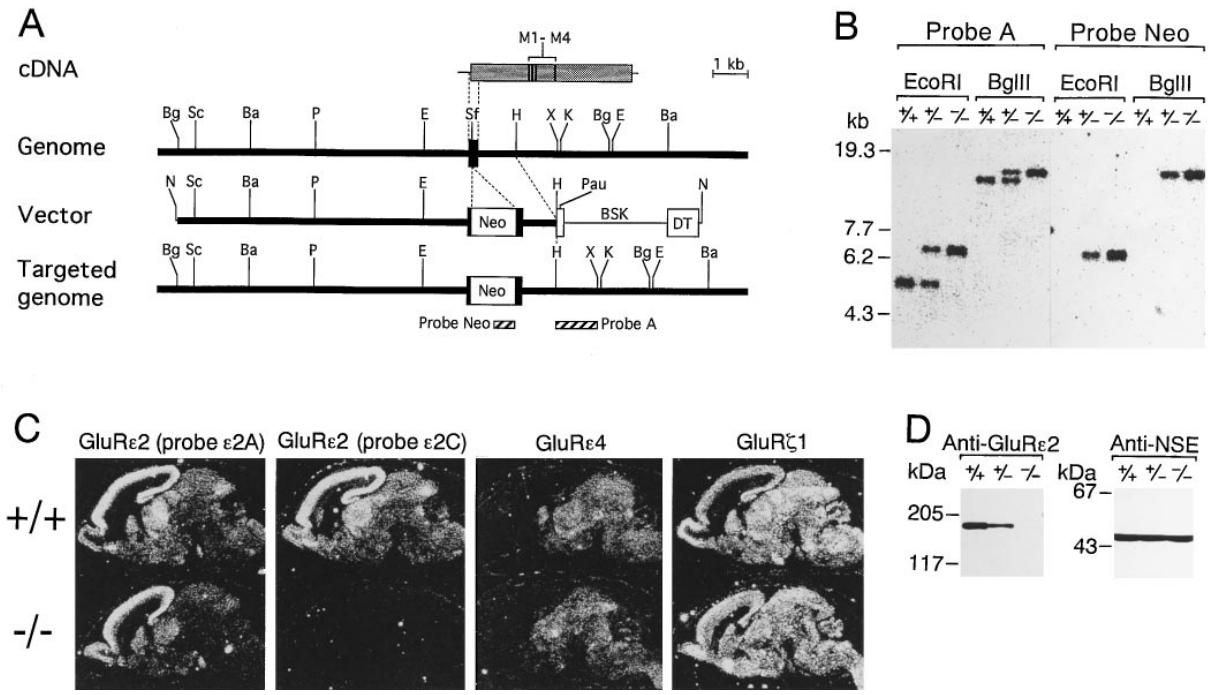

Figure 1. Targeted Disruption of the Mouse NMDA Receptor Channel ϵ2 Subunit Gene

(A) Schematic representations of GluRϵ2 cDNA, genomic DNA, targeting vector, and disrupted gene. BSK, plasmid pBluescript; DT, diphtheria toxin gene; M1–M4, four hydrophobic segments; Neo, neomycine-resistant gene; Pau, mRNA destabilizing and transcription pausing signals; Ba, BamHI; Bg, BglII; E, EcoRI; H, HindIII; K, KpnI; N, NotI; P, PstI, Sc, ScaI; Sf, SfiI; X, XbaI.

(B) Southern blot analysis of EcoRI- or BglII-digested genomic DNA.

(C) In situ hybridization analysis of parasagittal brain sections of the wild-type (+/+) and mutant (−/−) mice at P0.

(D) Western blot analysis of whole-brain proteins of the wild-type and mutant mice at P0 with anti-GluRϵ2 and anti-NSE antibodies.

responded only with retraction of the tongue to the same stimulation, and suckling-like movements were scarcely observed (Figure 2, −/−). We further compared the response to tactile stimulation of the oral cavity. Rhythmic tongue movements of more than three cycles were induced in the wild-type mice with high frequency (79%, 96 out of 122 trials; n = 5 animals), whereas the occurrence was rare in the mutant mice (9%, 17 out of 183 trials; n = 5 animals). These results strongly suggest that the sensory input does not effectively induce suckling movement in the mutant mice.

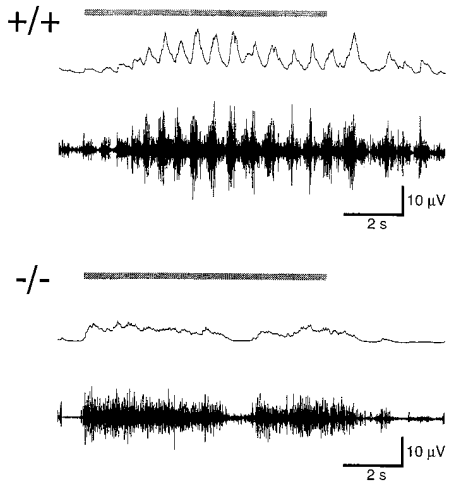

Figure 2. EMG Activity of the Tongue Induced by Tactile Stimulation

Stimulation by a light touch with a cannula evokes a rhythmic suckling movement of the tongue in the wild-type (+/+) mice at P0* but only tonic activities corresponding to retraction of the tongue in the mutant (−/−) mice. Upper traces, integrated EMG activities; lower traces, EMG recordings; horizontal bars above traces, duration of the stimulation.

Recovery by Hand Feeding

To examine whether the neonatal death of the ϵ2 subunit mutant mice is due to the lack of nutrition caused by the defect in suckling response or to other primary defects such as a respiration abnormality (as proposed for the ζ1 subunit mutant mice; Forrest et al., 1994; Li et al., 1994), we tried to feed newborn mice by hand. When milk was fed every 2–3 hr through a fine, soft tube inserted into the stomach, the newborn pups could survive. Genotyping of the pups reared for 2–3 days showed that there were 42 wild-type, 83 heterozygous, and 43 homozygous mutant mice, the ratio being close to 1:2:1. The pups grew normally, and their body weights after 2 days of hand feeding (+/+, 1.56 ± 0.03 g, n = 14; +/−, 1.52 ± 0.03 g, n = 20; −/−, 1.52 ± 0.03 g, n = 16) were comparable to those of the normal mice raised at the breast for 2 days (1.54 ± 0.07 g; n = 15). However, the mutant mice showed no suckling response even after 3 days of hand feeding (n = 9). We did not systematically study how long the mutant mice could grow by hand feeding, but 1 mutant mouse survived for 6 days.

These results clearly show that the primary cause of the neonatal death of the ε2 subunit mutant mice is the defect in the suckling response leading to the lack of nutrition. For further studies, we reared both the wild-type and mutant newborn mice by hand feeding, and their postnatal days are referred to with asterisks (e.g., P2* represents postnatal day 2 reared by hand feeding).

Failure of Neuronal Pattern Formation in the Brainstem Trigeminal Complex

The size and proportion of the brain of the mutant mice at P0 were similar to those of the wild-type mice (Figures 3A and 3B). By Nissl staining, laminae I, V, and VI were distinguishable in the cerebral cortex of both the wild-type and mutant mice (Figures 3C and 3E). The pyramidal and granule cells in the hippocampal formation were organized into a discrete layer in the Ammon's horn and dentate gyrus, respectively (Figures 3D and 3F). Similar histological features were observed between the wild-type and mutant mice in other brain regions, including olfactory bulb, superior colliculus, cerebellar cortex, cranial nerve nuclei, and inferior olivary nucleus, where the ε2 subunit mRNA was abundantly expressed at neonatal stages (Watanabe et al., 1992). Furthermore, the brain

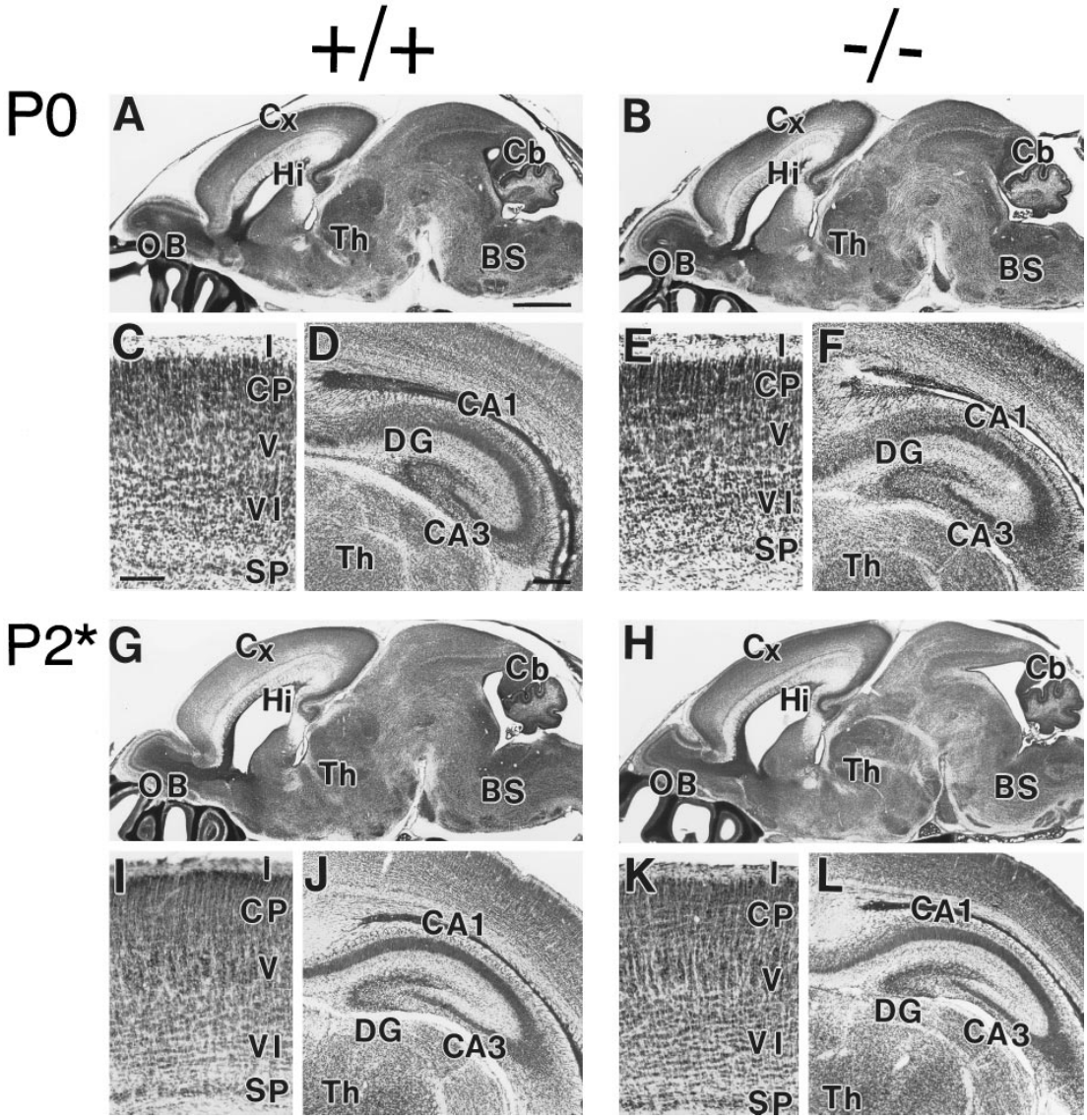

Figure 3. Nissl-Stained Brain Sections

(A and B) Parasagittal whole-brain sections of wild-type (A) and mutant (B) mice at P0.
(C and E) Cerebral cortex (parietal lobe) of wild-type (C) and mutant (E) mice at P0.
(D and F) Hippocampus of wild-type (D) and mutant (F) mice at P0.
(G and H) Parasagittal whole-brain sections of wild-type (G) and mutant (H) mice at P2*.
(I and K) Cerebral cortex (parietal lobe) of wild-type (I) and mutant (K) mice at P2*.
(J and L) Hippocampus of wild-type (J) and mutant (L) mice at P2*.
Bars, 1 mm (A), 200 μm (C), 100 μm (D).
BS, brainstem; CA1 and CA3, CA1 and CA3 fields of Ammon's horn; Cb, cerebellum; CP, cortical plate; Cx, cerebral cortex; DG, dentate gyrus; Hi, hippocampal formation; I, V, VI, cortical laminae I, V, and VI; OB, olfactory bulb; SP, subplate; Th, thalamus.

of the mutant mice developed during 2 days of hand feeding as did that of the wild-type mice, and no significant histological difference was observed between the two genotypes of mice (Figures 3G–3L).

Suckling behavior, such as nipple attachment and sucking movements, is regulated by complex interactions between sensory and motor neuronal pathways, which are linked to the central nervous system through the brainstem trigeminal complex (BSTC). In the BSTC, it is well established that the primary vibrissal afferent fibers interact with the secondary neurons and compose the discrete neural repeating units called barrelettes, which form an overall pattern homeomorphic to the pattern of the whiskers on the face of rodents (Belford and Killackey, 1979; Ma, 1991). The histoarchitecture of the barrelettes can be visualized by staining of mitochondrial enzymes (Belford and Killackey, 1979; Ma, 1991). Cytochrome oxidase histochemistry showed the formation of barrelettes in the spinal trigeminal nucleus of the wild-type mice at P0 (n = 12). In the mutant mice at P0, however, the staining was rather homogeneous, and no clear barrelette-like patches were observed (n = 10).

Cytochrome oxidase staining of the spinal trigeminal nucleus of the wild-type mice at P2* revealed more clearly discernible barrelettes consisting of five distinct rows of patches corresponding to the five rows of whiskers (n = 13; Figure 4A). The barrelette patches were separated from each other by septa with little staining. In the nucleus of the mutant mice at P2*, however, the staining was still diffuse, and barrelette-like patches were missing (n = 12; Figure 4D). The staining intensity of the mutant nucleus was lower than that of the wild-type patches, but was higher than that of the wild-type septa. The strength of cytochrome oxidase staining was comparable between the wild-type and mutant mice in other regions, including the hypoglossal nucleus, the inferior olive, the facial motor nucleus, and the trigeminal motor nucleus. These results show that the formation of chemoarchitectural barrelettes is impaired in the ϵ2 subunit mutant mice.

Impairment of Primary Sensory Terminal Clustering

The cytochrome oxidase staining represents primarily mitochondria in the primary afferent terminals and the dendrites of the secondary neurons in the barrelettes (Wong-Riley and Welt, 1980; Wong-Riley, 1989; Ma, 1991). To examine the connectivity, somatotopy, and terminal arborization of the primary afferent fibers, we labeled a limited number of the trigeminal primary sensory nerves and the facial nerves by injecting cholera toxin B subunit (CTB; Shen and Semba, 1994) into a single vibrissa (vibrissa B1) follicle on the right whisker pad of mice at P0. Two days after injection, a number of serial coronal sections were prepared to visualize the labeled neurons and fibers by immunohistochemistry with anti-CTB antibody. Some of the sections were processed for cytochrome oxidase histochemistry.

In the subnucleus interpolaris of the spinal trigeminal nucleus in the wild-type mice, the terminal arbors of the primary sensory neurons (trigeminal ganglion cells) were distributed in the ventrolateral region and formed distinct clusters (Figure 4B, asterisk and triangles). When compared with the adjacent section processed for cytochrome oxidase histochemistry (Figure 4A), one of the terminal clusters coincided with the histochemical barrelette corresponding to vibrissa B1 injected with CTB (Figures 4A and 4B, asterisks). Additional terminal clusters also coincided with the histochemical barrelettes corresponding to vibrissae around vibrissa B1 (Figures 4A and 4B, triangles). The discrete clusters of the labeled terminals consistently occupied a similar nuclear region in sections cut at various rostrocaudal levels of the subnucleus (Figure 4C).

In the mutant nucleus, CTB-labeled terminal arbors were also found in the ventrolateral region, indicating that the connectivity and somatotopy of the primary afferent fibers were largely preserved. However, terminal arbors were distributed diffusely, and no distinct clustering was observed over the region at various rostrocaudal levels in the mutant mice (Figures 4E and 4F). The difference in the terminal arborization between the wild-type and mutant mice was reproducibly observed (+/+, n = 4; −/−, n = 3). No significant histological differences in size and location of the trigeminal ganglion and in shape and density of the ganglion cells were observed between the wild-type and mutant mice (data not shown). These results suggest that the deprivation of the ϵ2 subunit impairs the vibrissa-related clustering of the primary afferent terminals in the BSTC, although the nerve fibers project to the trigeminal nucleus with grossly preserved somatotopy.

The nasolabial muscle adjacent to the vibrissa injected with CTB is innervated by motor neurons in the lateral and dorsolateral subnuclei of the facial nucleus (Ashwell, 1982). CTB-labeled motor neurons were localized in these subnuclei of the facial nucleus in both wild-type and mutant mice (Figures 4G and 4I). Furthermore, there were no significant differences between the wild-type and mutant mice in the shape of the motor neurons and the genu formation of the axons (Figures 4G–4J).

In situ hybridization analysis showed that the ϵ2 subunit mRNA was abundantly expressed in the trigeminal nucleus of the wild-type mice, but was absent in the mutant mice (Figures 5B and 5G). In addition to the ζ1 subunit mRNA, the ϵ4 subunit mRNA was also expressed in the nucleus, whereas weak or little expression of the ϵ1 and ϵ3 subunit mRNAs was found (Figures 5A, 5C–5F, and 5H–5J).

Synaptic Plasticity in the Hippocampus at Neonatal Stages

Since little information is available for plasticity of synaptic transmission in mice at neonatal stages, even in the hippocampus, we first examined whether LTP or LTD can be induced in normal mice at P2–P3 by recording extracellular field potentials in the CA1 region of hippocampal slices using standard techniques (Manzoni et al., 1994). We used three protocols to induce LTP. Tetanic stimulation at 100 Hz for 1 s repeated twice at an interval of 10 s failed to cause synaptic potentiation in all six slices (95.1% ± 11.5% of control). LTP could be induced with the same stimulation in mice at P15–P16 (data not shown). We also used θ bursts (4 pulses at 100 Hz repeated 20 times at an interval of 200 ms), which were reported to be more efficient for inducing LTP than tetanic stimulation (Larson et al., 1986), but again no potentiation was observed (99.4% ± 2.6% of control; n =

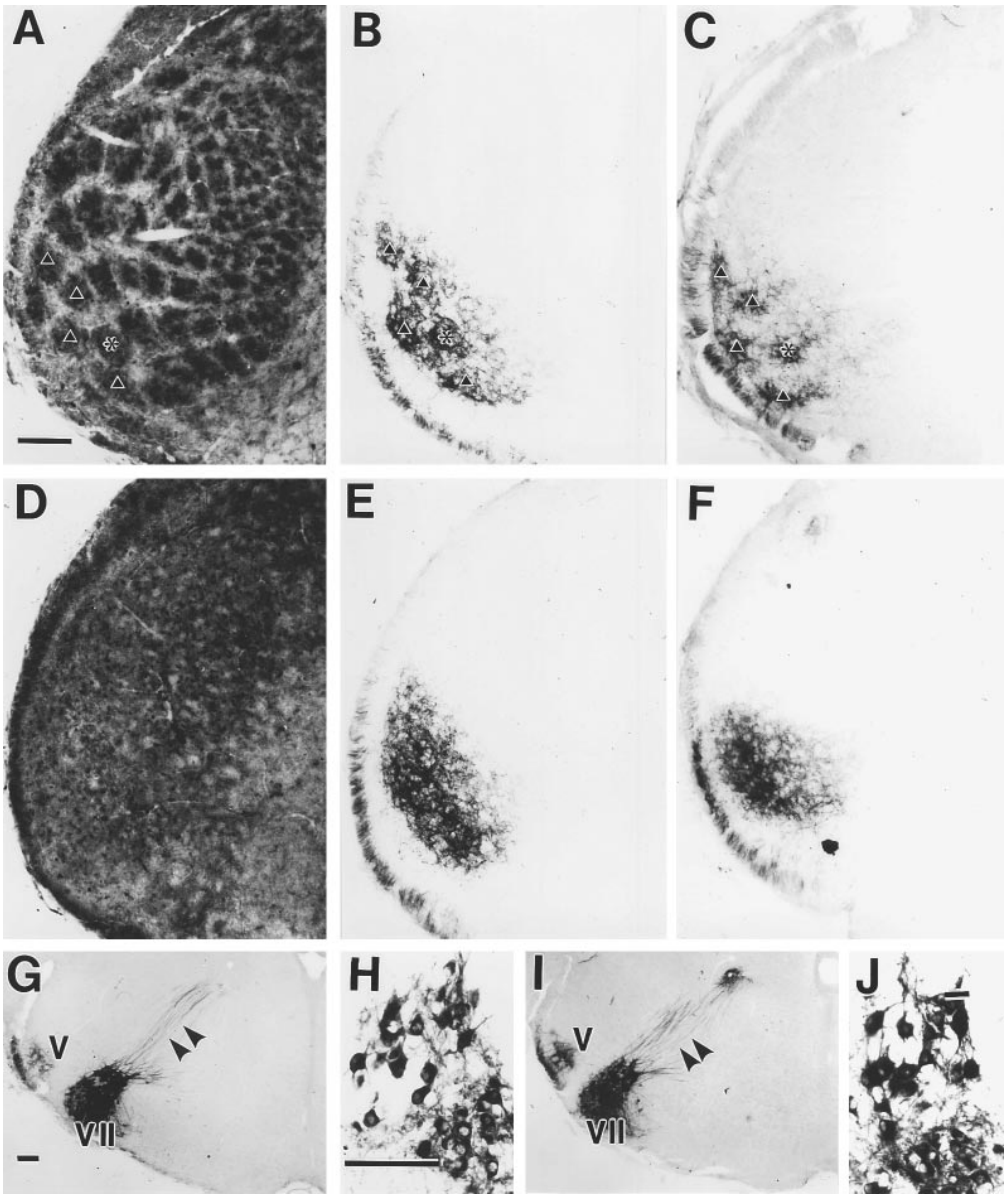

Figure 4. Cytochrome Oxidase Histochemistry of Whisker-Related Barrelettes and Immunohistochemistry of CTB-Labeled Primary Afferent Fibers in the Brainstem

(A and D) Cytochrome oxidase histochemistry at the spinal trigeminal nucleus (subnucleus interpolaris) of wild-type (A) and mutant (D) mice at P2*. Five distinct rows of patches (barrelettes), corresponding to whiskers, are present in the wild-type trigeminal nucleus but are absent in the mutant trigeminal nucleus. An asterisk and arrowheads indicate the barrelettes, which correspond to the clusters of afferent fibers labeled by CTB in (B) and (C).

(B, C, E, and F) CTB labeling of primary afferent fibers of trigeminal nerves at the spinal trigeminal nucleus of the wild-type (B and C) and mutant (E and F) mice at P2*. Immunohistochemistry with anti-CTB antibody was done using the serial sections of (A) and (D). Sections (B) and (E) are adjacent to (A) and (D), respectively, while sections (C) and (F) are 140 μm caudal to (B) and (E), respectively. Note that the terminal arbors of afferent fibers labeled by CTB are organized into clusters (an asterisk and triangles) in the wild-type trigeminal nucleus (B and C) but are distributed diffusely over the mutant nucleus (E and F). The asterisk indicates the cluster corresponding to vibrissa B1, around which CTB was injected.

(G and I) CTB labeling of motor neurons in the facial nucleus in the pons of wild-type (G) and mutant (I) mice at P2*. Transported CTB is found in the cell bodies and axons of motor neurons in the facial nucleus (VII). The axons (arrowheads) run dorsomedially toward the geniculum of the facial nerve. Labeling is also detected in the subnucleus oralis of the spinal trigeminal nucleus (V).

(H and J) CTB labeling of motor neurons in the facial nucleus of wild-type (H) and mutant (J) mice at higher magnification.

Bars, 100 μm (A and H), 200 μm (G).

4). Since synaptic inputs are weaker in young animals, these protocols using high frequency stimulation may not cause sufficient depolarization of postsynaptic cells to relieve Mg^{2+} block of the NMDA receptor channel. To circumvent this possible problem, we made whole-cell voltage-clamp recordings from CA1 pyramidal cells and

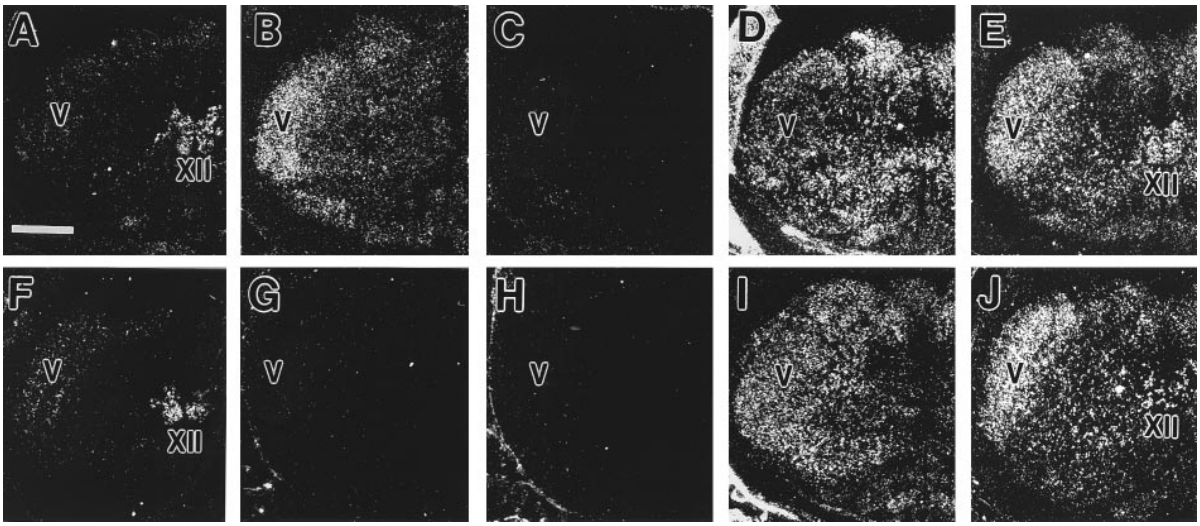

Figure 5. In Situ Hybridization Analysis of Coronal Sections through the Brainstem

(A–E) Expression of the ϵ1 (A), ϵ2 (B), ϵ3 (C), ϵ4 (D), and ζ1 (E) subunit mRNAs in the brainstem of wild-type mice at P0.
(F–J) Expression of the ϵ1 (F), ϵ2 (G), ϵ3 (H), ϵ4 (I), and ζ1 (J) subunit mRNAs in the brainstem of mutant mice at P0.
V, the trigeminal nucleus; XII, the hypoglossal nucleus. Bar, 500 μm.

paired electrical stimulation (80 times at 2 Hz) with postsynaptic depolarization to 0 mV. With this protocol, we have been able to induce LTP reliably in older animals (Manabe et al., 1993). However, we again failed to observe LTP, and the pairing resulted in a small depression rather than potentiation (80.3% ± 24.7% of control; n = 4). Thus, in our conditions, LTP was absent in normal mice at P2–P3, in accordance with the previous reports (Harris and Teyler, 1984; Muller et al., 1989; Izumi and Zorumski, 1995).

On the other hand, prolonged low frequency stimulation (1 Hz for 15 min) of afferent fibers produced robust LTD in slices from normal mice at P2–P3 (79.0% ± 1.9% of control; n = 8). As shown in Figure 6, induction of LTD by prolonged low frequency stimulation was completely blocked by D-2-amino-5-phosphonovaleric acid (D-APV), a competitive NMDA receptor antagonist, in all slices examined (101.3% ± 1.8% of control; n = 5). LTD was induced by the same conditioning after washout of D-APV in all slices (77.8% ± 2.9% of control). Thus, NMDA receptor channel–dependent LTD is already present in the hippocampus at neonatal stages.

Lack of Synaptic NMDA Responses and LTD in the Hippocampus of the ϵ2 Subunit Mutant Mice

We then studied basic properties of excitatory synaptic transmission and LTD in the CA1 region of hippocampal slices prepared from the ϵ2 subunit mutant mice. All the electrophysiological experiments using mutant mice were done in a completely blind fashion. Non-NMDA receptor channel–mediated excitatory postsynaptic potentials (EPSPs) were recorded in a normal extracellular medium, and there was no clear difference in the properties of EPSPs between the wild-type and mutant mice at P0 (n = 6 each) and at P2*–P3* (+/+, n = 8; −/−,

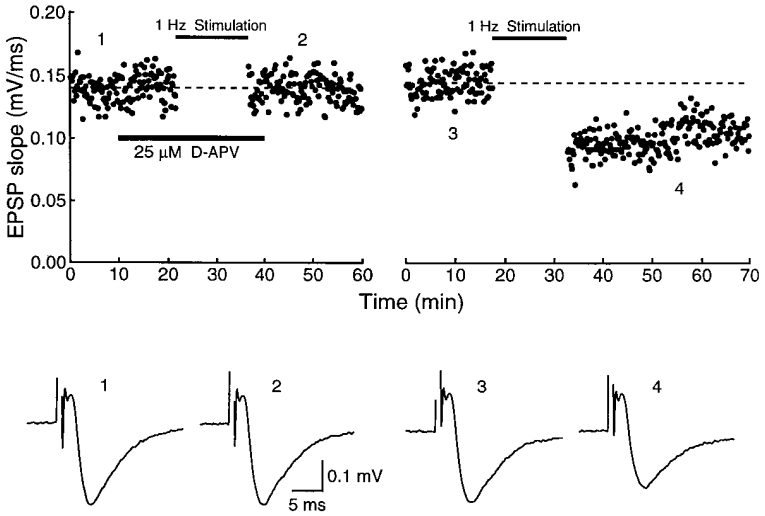

Figure 6. An Example of Homosynaptic LTD in Normal Mice

EPSPs were recorded with extracellular field potential recordings in the CA1 region of the hippocampus. Prolonged low frequency stimulation (1 Hz for 15 min) failed to induce any synaptic depression in the presence of 25 μM D-APV. In the same input, the same stimulation induced LTD 60 min after starting washout of D-APV. Traces represent averages of ten consecutive EPSPs obtained at the times indicated on the upper panel. The broken lines on the upper panel indicate the average value of the EPSP slope during the control period.

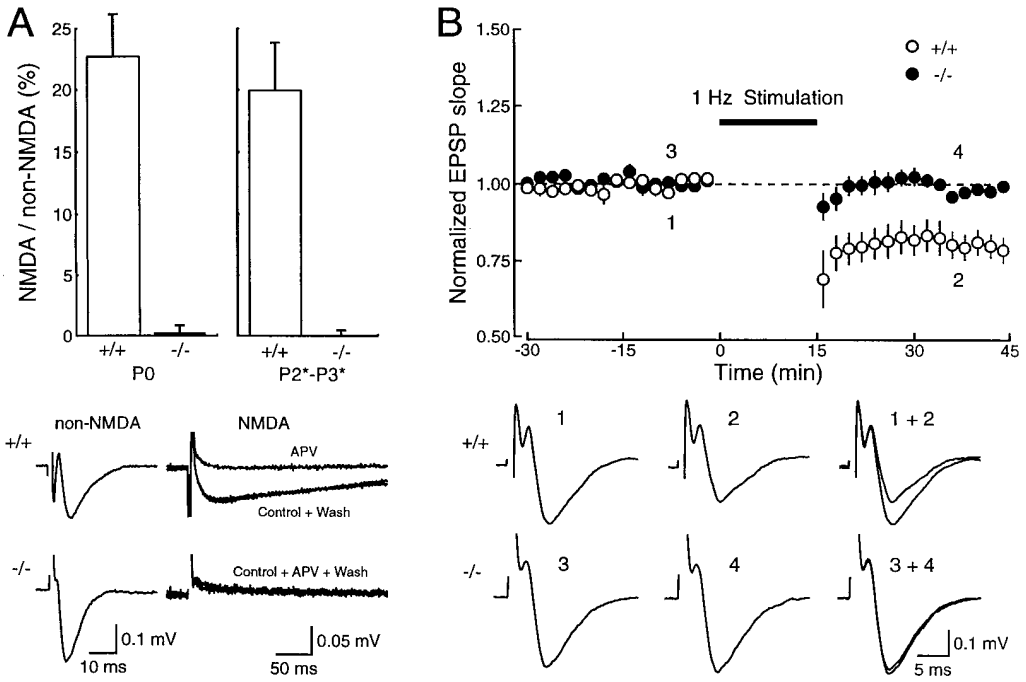

Figure 7. Synaptic NMDA Responses and LTD in Mutant Mice

(A) Ratio of the amplitudes of the NMDA components to those of the non-NMDA components of EPSPs in the wild-type and mutant slices. Slices from the mutant mice at P0 (upper left) and at P2*–P3* (upper right) lack the NMDA receptor channel–mediated synaptic response. Traces represent averages of ten consecutive EPSPs recorded in a slice from a wild-type or mutant mouse at P3*. Although normal non-NMDA EPSPs were observed, no NMDA component was present in the mutant slice.

(B) Summary graph of the LTD experiments with mice at P2*–P3*. Prolonged stimulation of afferent fibers at 1 Hz induced LTD in wild-type slices (n = 8; open circles), while the same stimulation failed to induce LTD in mutant slices (n = 5; closed circles). Traces represent averages of ten consecutive EPSPs obtained at the times marked by the numbers on the upper panel.

n = 5). NMDA receptor channel–mediated EPSPs were measured in a Mg^{2+}-free medium containing 20 μM 6-cyano-7-nitroquinoxaline-2,3-dione (CNQX), a competitive non-NMDA receptor antagonist. NMDA components of the synaptic potentials were clearly detected in slices from the wild-type mice at P0 (n = 6) and at P2*–P3* (n = 8), which were completely abolished when 50 μM D-APV was perfused and recovered after washout of the antagonist. On the other hand, there was no APV-sensitive response in slices from the mutant mice at P0 (n = 6) and at P2*–P3* (n = 5) (Figure 7A). These results show that there are no functional synaptic NMDA receptor channels at neonatal stages in the ε2 subunit mutant mice.

Prolonged low frequency stimulation of afferent fibers produced robust LTD in slices from the wild-type mice at P2*–P3* (n = 8; Figure 7B), as in those from the normal mice at P2–P3. In contrast, no long-lasting depression was observed in any of slices from mutant littermates at P2*–P3* (n = 5; Figure 7B). These results provide direct evidence that NMDA receptor channel activation is essential for LTD induction in the hippocampus, in agreement with previous reports showing that LTD induction in the rat hippocampus at P6 and later stages is blocked by an NMDA receptor antagonist (Dudek and Bear, 1992; Mulkey and Malenka, 1992).

Discussion

Using antagonists selective for the NMDA receptor channel, it has been shown that the NMDA receptor channel plays a key role in some forms of LTP and LTD of synaptic transmission (Bliss and Collingridge, 1993; Malenka and Nicoll, 1993) and is involved in neuronal pattern formation (Cline et al., 1987; Kleinschmidt et al., 1987; see also Miller et al., 1989). These findings raise an intriguing possibility that similar molecular mechanisms may underlie learning and memory acquisition and the activity-dependent synapse refinement during development. However, studies with antagonists or mice defective in the common ζ1 subunit cannot exclude the possibility that different types of NMDA receptor channels with distinct subunit compositions and functional properties may play different roles, since recent studies have revealed the molecular and functional diversity of the NMDA receptor channel, and the multiple ε subunits are major determinants of this diversity (Mishina et al., 1993; Seeburg, 1993; Mori and Mishina, 1995). There remains a question as to whether the same or different NMDA receptor channels play key roles in synaptic plasticity and neuronal pattern formation during development.

In the embryonic brains, two ε subunits, ε2 and ε4, are expressed (Watanabe et al., 1992). It is not known which ε subunit is responsible for neuronal pattern formation. The ε4 subunit is strongly expressed in the diencephalon and the brainstem at the embryonic stages, and its expression is greatly decreased at postnatal stages (Watanabe et al., 1992). The ε4/ζ1 NMDA receptor channel is less sensitive to Mg^{2+} block than the ε1/ζ1 and ε2/ζ1 channels and exhibits a longer decay time constant of channel opening (Mishina et al., 1993; Seeburg, 1993; Mori and Mishina, 1995). From these points

of view, one may infer that the ε4 subunit can be responsible for neuronal pattern formation during development and that the other ε subunits are involved in synaptic plasticity in the adult brain. On the other hand, the ε2 subunit is strongly expressed in the entire embryonic brain, but is restricted to the forebrain in the adult (Watanabe et al., 1992). The ε2/ζ1 channel is highly sensitive to Mg^{2+} block (Kutsuwada et al., 1992; Monyer et al., 1992). Based on the strong expression in the adult hippocampus and neocortex and high sensitivity to Mg^{2+} block, we have proposed that the ε2 subunit, together with the ε1 subunit, plays a role in synaptic plasticity (Kutsuwada et al., 1992; Mishina et al., 1993).

In the present investigation, we have provided experimental evidence that the ε2 subunit of the NMDA receptor channel does play a critical role in trigeminal neuronal pattern formation and hippocampal LTD at neonatal stages. On the other hand, mice defective in the ε4 subunit, the other embryonic ε subunit, develop normal whisker-related neuronal patterns in the BSTC, although they show reduced spontaneous behavioral activity in an open field (Ikeda et al., 1995).

The ε2 Subunit of the NMDA Receptor Channel Is Indispensable

The neonatal death of the ε2 subunit mutant mice demonstrates that the ε2 subunit of the NMDA receptor channel is indispensable for development. Of five subunits of the NMDA receptor channel, the ε2, ε4, and ζ1 subunits are expressed in the embryonic brain (Watanabe et al., 1992). The disruption of the ζ1 subunit gene is also lethal (Forrest et al., 1994; Li et al., 1994). These results indicate that both the ε subunit family and the ζ subunit family are essential for in vivo function of the NMDA receptor channel.

In addition to the ε2 and ζ1 subunit mRNAs, ε4 subunit mRNA is expressed in the BSTC, where the barrelette structure formation is impaired in the ε2 subunit mutant mice. The ε4 subunit mutant mice are viable and develop the barrelette structure normally (Ikeda et al., 1995). Thus, it is surprising that the disruption of the ε2 subunit alone is lethal. These observations suggest that within the subfamily the ε4 subunit does not compensate for the ε2 subunit. The ε4 subunit is significantly different in functional properties, such as Mg^{2+} sensitivity, from the ε2 subunit (Mishina et al., 1993; Seeburg, 1993; Mori and Mishina, 1995). Thus, failure of the ε4 subunit to compensate for the lack of the ε2 subunit in vivo may be ascribed to the qualitative difference in the functional properties of the two ε subunits. Alternatively, there may be quantitative differences. At least in the Xenopus oocyte expression system, channel activity of the ε4/ζ1 channel is much lower than that of the ε2/ζ1 channel (Ikeda et al., 1992; Kutsuwada et al., 1992). Although the exact mechanism remains to be established, our results clearly show that the in vivo functions of the respective ε subunits, molecular determinants of the NMDA receptor channel diversity, are distinct.

Suckling Response and Neuronal Pattern Formation

Rescue of the ε2 subunit mutant mice from neonatal death by hand feeding clearly shows that the primary cause of their neonatal death is a nutrition deficiency due to the defect of the suckling response. The ζ1 subunit mutant mice were reported to show similar phenotypes (i.e., no milk in their stomach and death 8–20 hr after birth), but neonatal death of the ζ1 subunit mutant mice was ascribed to a respiratory failure, though not proven (Forrest et al., 1994; Li et al., 1994).

We have also found that the formation of barrelettes, the whisker-related neural structures, is impaired in the BSTC of the ε2 mutant mice, despite the expression of the ε4 subunit in that region, as is the case for the ζ1 subunit mutant mice (Li et al., 1994). The barrelette hollows are the principle neuropil region in which primary afferents and their target neurons in the trigeminal nucleus interact (Bates and Killackey, 1985; Ma, 1991; Chiaia et al., 1992). CTB labeling of the primary sensory neurons shows that their arbors reach the trigeminal complex but fail to form distinct clusters in the ε2 subunit mutant mice. The ε2 and ζ1 subunit mRNAs are expressed in the embryonic BSTC when neurogenesis occurs (Erzurumlu and Jhaveri, 1992; Watanabe et al., 1992), whereas the trigeminal ganglion expresses only the ζ1 subunit mRNA (Watanabe et al., 1994b). Thus, loss of the ε2 subunit of the NMDA receptor channel in the postsynaptic trigeminal nucleus may result in the failure of refinement of the primary afferent terminals. We speculate that such a failure in synapse refinement might underlie the impairment of barrelette structure formation and suckling response.

LTD at Neonatal Stages

We examined the plasticity of synaptic transmission in the CA1 region of the hippocampus in mice at neonatal stages. No significant LTP was induced by three protocols in normal mice at P2–P3. These results are in accordance with previous reports on the absence of LTP in the rat hippocampus at P1–P4, P7–P9, and P9 (Harris and Teyler, 1984; Muller et al., 1989; Izumi and Zorumski, 1995), although it cannot be excluded that other protocols might be able to induce LTP in animals at this age. On the other hand, we found that prolonged low frequency stimulation gave rise to homosynaptic LTD of excitatory synaptic transmission in the hippocampus at P2–P3. Our results thus extend the observations that LTD is more reliably induced in younger rats (P6–P27) and that its appearance precedes that of LTP in the rat hippocampus (Mulkey and Malenka, 1992; Dudek and Bear, 1993). LTD induced by prolonged low frequency stimulation was completely blocked by D-APV. Thus, the LTD we have been looking at in this study is pharmacologically similar to that in older animals mediated by NMDA receptor activation (Dudek and Bear, 1992; Mulkey and Malenka, 1992). Our finding is in contrast to a recent report that LTD in neonatal rats (P3–P7), a stage before the development of LTP, is fundamentally different from that in older animals (Bolshakov and Siegelbaum, 1994). These observations, however, do not necessarily exclude each other if there are multiple mechanisms for LTD at neonatal stages. Whole-cell patch-clamp recordings were used in the study by Bolshakov and Siegelbaum (1994), and their LTD induction protocol (5 Hz for 3 min) was different from ours. Thus, it might be possible that their conditions preferentially

induce NMDA receptor channel–independent LTD, which was not observed in this study.

Impairment of LTD

At neonatal stages, the ε2 and ζ1 subunit mRNAs are strongly expressed in the hippocampus, while the expression of the ε1 subunit mRNA is just starting (Watanabe et al., 1992). The lack of measurable synaptic NMDA responses in the hippocampal slices of the ε2 subunit mutant mice suggests that the ζ1 subunit alone is not sufficient for the formation of functional NMDA receptor channels in vivo. Consistent with this view, highly active NMDA receptor channels are formed in vitro only when both the ε and ζ subunits are expressed together (Ikeda et al., 1992; Kutsuwada et al., 1992; Meguro et al., 1992; Monyer et al., 1992). For example, the current response of the heteromeric ε2/ζ1 NMDA receptor channel is more than two orders of magnitude larger than that of the homomeric ζ1 channel in a Xenopus oocyte expression system. Furthermore, most brain regions express both the ε and ζ subunit mRNAs of the NMDA receptor channel, and no NMDA receptor channel responses are detected in the mature cerebellar Purkinje cells, which express the ζ1 subunit but none of the ε subunits (Quinlan and Davies, 1985; Perkel et al., 1990; Watanabe et al., 1992, 1994a; Brose et al., 1993; Monyer et al., 1994).

We have shown that LTD in the hippocampus is deficient in the ε2 subunit mutant mice. Our previous study indicates that NMDA receptor channel current and LTP in the hippocampus and spatial learning are significantly decreased in the ε1 subunit mutant mice (Sakimura et al., 1995). Residual LTP in the hippocampus of the ε1 subunit mutant mice is most likely mediated by the ε2 subunit, since the ε1 and ε2 subunits are strongly expressed in the adult hippocampus. These results with gene knockout mice provide experimental evidence for our proposal, based on the sensitivity to Mg^{2+} block and distribution, that the ε1 and ε2 subunits of the NMDA receptor channel play a role in the synaptic plasticity (Kutsuwada et al., 1992; Mishina et al., 1993). Our finding that the ε2 subunit is essential for both LTD in the hippocampus and neuronal pattern formation in the trigeminal nucleus suggests that both processes share common molecular machinery. It remains to be established whether these processes are causally related.

Experimental Procedures

Production of the GluRε2 Mutant Mice

Genomic DNA from C57BL/6 mouse liver was digested by BglII and size-fractionated by 10%–38% sucrose density gradient centrifugation. Approximately 10–13 kb genomic DNA fragments were inserted into BamHI-digested λDASHII phage vector (Stratagene). The genomic library was screened with the 392 bp SalI–NcoI fragment from pGRU9 (Kutsuwada et al., 1992), and the 12.6 kb XbaI fragment from a positive clone λGRE2Bg1 was inserted into the XbaI site of pBluescript II KS(−) to yield pGRE2X1. The 2.7 kb EcoRI–HindIII fragment from pGRE2X1, carrying the 429 bp exon with the initial methionine codon of the ε2 subunit, was ligated with the 2.9 kb EcoRI–HindIII fragment from pBluescript II KS(−) to yield pGRE2EH1. The 1.3 kb EcoRI–BamHI fragment from pGK2Neo (Yagi et al., 1993a) and SfiI-digested pGRE2EH1 were blunted and ligated to yield pGRE2N1. The 7.1 kb EcoRI fragment from pGRE2X1 and EcoRI-digested pGRE2N1 were ligated to yield pGRE2N2. The 11.1 kb NotI–XhoI fragment from pGRE2N2 and the 4.0 kb NotI–XhoI fragment from pPauDT1 (Sakimura et al., 1995) were ligated to yield pTVGRε2.

TT2 embryonic stem cells (Yagi et al., 1993b) were transfected with NotI-cleaved pTVGRε2 by electroporation using a Bio-Rad Gene Pulser. Three targeted clones were identified by G418 selection, polymerase chain reaction (PCR), and Southern blot hybridization, the frequency of homologous recombination being 0.2% of G418-resistant colonies. Cells of three targeted clones were injected into 8-cell embryos of ICR mice to produce chimeras. Chimeras were mated to C57BL/6 mice, and those derived from clones P60 and T43 transmitted the mutation through the germline.

Heterozygous males and females were mated overnight. Next morning, the females were checked for vaginal plug, and the day was referred to as embryonic day 0 (E0). The females were delivered between E19.0 and E19.5. Breeding and maintenance were carried out under standard mouse husbandry procedures.

Southern Blot, In Situ Hybridization, and Western Blot Analyses

Genotyping and functional analyses of mice were done in a completely blind fashion. Southern blot analysis of tail DNA was done using the 1.2 kb HindIII–XbaI fragment from pGRE2X1 and the 0.6 kb PstI fragment from pGK2Neo. In situ hybridization and Western blot analyses were carried out as described (Watanabe et al., 1992; Araki et al., 1993), except that GluRε2 protein was detected by chemiluminescence (Amersham). Oligonucleotide probes ε2A and ε2C are complementary to the nucleotide residues −96 to −52 and −45 to −2, respectively, of the ε2 subunit cDNA (Kutsuwada et al., 1992). Antibodies against GluRε2 and NSE were previously prepared (Sakimura et al., 1980, 1995).

Rearing by Hand Feeding

Newborn pups were weighed and kept in a moist chamber at 34°C ± 1°C. For hand feeding, a fine polyethylene tube with an outer diameter of 0.5 mm and a silicon tube cap on the tip was inserted into the stomach, and milk was fed through the tube from a calibrated syringe. To avoid regurgitation, 15–30 μl of homogenized cow's milk with 0.65 g/ml of infant formula for human neonates (Neomilk P. ai, Snow Bland, Tokyo, Japan) was given at 2 hr intervals in the initial 2–3 feedings, and subsequently 30–60 μl of milk was fed at 3 hr intervals. The final concentrations of protein and fat were 5.4% and 8.0%, respectively. Pups were stimulated for urination and defecation after every feeding by lightly touching the perineal region with wet tissue paper.

Suckling Response

The suckling behavior consists of three components: nipple attachment, in which the pup takes the nipple between the jaws and into the mouth; rhythmic suckling, a low frequency, rhythmic movement of the jaws and tongue while attached to the nipple; and the stretch response during the milk letdown, which consists of elongation of the body, arching of the back, waving of the tail, and rapid, rhythmic contraction of the jaw muscle (Westneat and Hall, 1992). The rhythmic suckling movement can be produced by mechanical stimulation to the lips. Newborn pups were examined for suckling response by stimulating the upper lip with a soft cannula.

EMG was recorded from the tongue of mice at P0* and P1*. Under anesthesia, a pair of fine-wire electrodes (0.05 mm diameter Teflon-coated tungsten wire) was inserted into the tongue from the ventral surface posterior to the mandibular symphysis and fixed with cyanoacrylate glue to the skin for monitoring the EMG activity of the tongue. After recovery from anesthesia, the tongue was stimulated by a light touch with a cannula (constructed from 1 mm diameter polyethylene tube, one end of which was rounded with heat) inserted into the mouth. A binocular microscope (M610, WILD) was used to confirm the stimulation site as well as to observe the induced tongue movements. EMG was preamplified with a high impedance probe (JH-220J, Nihon Kohden), amplified 1000 times with AB-651J (Nihon Kohden), and filtered at 100–3000 Hz. EMG signals were displayed on a digital storage oscilloscope (CS-8010, KENWOOD) and a thermal array recorder (WR7600, GRAPHTEC) and were stored on a DAT tape recorder (RD-180T, TEAC).

Histology

Mice at P0 and P2* were fixed by transcardial perfusion with 4% paraformaldehyde in 0.1 M phosphate buffer (pH 7.4). After cryoprotection, sagittal and coronal sections (20 μm thickness) were prepared by a cryostat and stained with toluidine blue.

CTB (1 mg/ml) was subcutaneously injected around vibrissa B1 on the right whisker pad of mice at P0 (0.3 μg per mouse). At P2*, the injected mice were sacrificed by transcardial perfusion with Zamboni's solution (Stefanini et al., 1967). Brains were removed from skulls, cryoprotected with 30% sucrose in 0.1 M phosphate buffer (pH 7.4), and cut into sections (20 μm thickness) in the coronal plane by a cryostat. Sections were reacted with anti-CTB antibody (List Biological Lab.) at a dilution of 1:10,000 and stained by the ABC method (Hsu et al., 1981) to visualize the transported CTB.

Cytochrome oxidase histochemistry was carried out as described (Wong-Riley, 1979). In brief, sections adjacent to those used for CTB immunohistochemistry were treated at 37°C for 12–24 hr with a solution containing 3 mg of cytochrome C, 5 mg of 3,3′-diaminobenzidine, and 450 mg of sucrose in 10 ml of 0.1 M phosphate buffer (pH 7.4).

Electrophysiology

Horizontal whole-brain slices (400 μm thick) were prepared from mice at P0, P2–P3, and P2*–P3* and placed in a holding chamber for at least 1 hr. A single slice, which contained transverse hippocampal slices conventionally used for electrophysiology, was then transferred to the recording chamber and submerged beneath a continuously perfusing medium that had been saturated with 95% O_2, 5% CO_2. The medium contained 119 mM NaCl, 2.5 mM KCl, 1.3 mM $MgSO_4$, 2.5 mM $CaCl_2$, 1.0 mM NaH_2PO_4, 26.2 mM $NaHCO_3$, 11 mM glucose, and 0.1 mM picrotoxin. All the experiments were done at room temperature (22°C–25°C). Field potential recordings were made in the CA1 region of the hippocampus with a glass pipette filled with 3 M NaCl. To evoke synaptic potentials, we delivered stimuli at 0.1 Hz with a bipolar tungsten electrode placed in the stratum radiatum. Field EPSPs were recorded with an Axopatch-1D amplifier, filtered at 1 kHz, digitized at 2–5 kHz, and stored on an IBM AT compatible computer. To evoke the NMDA receptor–mediated EPSP, Mg^{2+} was removed from the medium and 20 μM CNQX was added. When non-NMDA and NMDA components of the EPSP were compared, amplitudes of the responses were measured. For non-NMDA EPSPs, amplitudes were calculated by averaging a 5 ms window around the peak. For NMDA EPSPs, amplitudes were measured by averaging the values 40–50 ms after the stimulus in the control medium and subtracting those in the presence of D-APV. In LTD experiments, initial slopes of the EPSP were measured. A single slice was used in each mouse.

Acknowledgments

We thank N. Takeda for help in the preparation of chimeric mice and R. Ochi for her valuable advice on cytochrome oxidase staining. This investigation was supported, in part, by research grants from the Ministry of Education, Science, and Culture of Japan, the Ministry of Health and Welfare of Japan, the Yamanouchi Foundation, the Naito Foundation, and the Uehara Memorial Foundation.

The costs of publication of this article were defrayed in part by the payment of page charges. This article must therefore be hereby marked *"advertisement"* in accordance with 18 USC Section 1734 solely to indicate this fact.

Received August 28, 1995; revised October 30, 1995.

References

Araki, K., Meguro, H., Kushiya, E., Takayama, C., Inoue, Y., and Mishina, M. (1993). Selective expression of the glutamate receptor channel δ2 subunit in cerebellar Purkinje cells. Biochem. Biophys. Res. Commun. *197*, 1267–1276.

Ascher, P., and Nowak, L. (1986). Calcium permeability of the channels activated by *N*-methyl-D-aspartate (NMDA) in isolated mouse central neurones. J. Physiol. *377*, 35.

Ashwell, K.W. (1982). The adult mouse facial nerve nucleus: morphology and musculotopic organization. J. Anat. *135*, 531–538.

Bates, C.A., and Killackey, H.P. (1985). The organization of the neonatal rat's brainstem trigeminal complex and its role in the formation of central trigeminal patterns. J. Comp. Neurol. *240*, 265–287.

Belford, G.R., and Killackey, H.P. (1979). Vibrissae representation in subcortical trigeminal centers of the neonatal rat. J. Comp. Neurol. *183*, 305–322.

Bliss, T.V.P., and Collingridge, G.L. (1993). A synaptic model of memory: long-term potentiation in the hippocampus. Nature *361*, 31–39.

Bolshakov, V.Y., and Siegelbaum, S.A. (1994). Postsynaptic induction and presynaptic expression of hippocampal long-term depression. Science *264*, 1148–1152.

Brose, N., Gasic, G.P., Vetter, D.E., Sullivan, J.M., and Heinemann, S.F. (1993). Protein chemical characterization and immunocytochemical localization of the NMDA receptor subunit NMDA R1. J. Biol. Chem. *268*, 22663–22671.

Capecchi, M.R. (1989). Altering the genome by homologous recombination. Science *244*, 1288–1292.

Chiaia, N.L., Bennett-Clarke, C.A., and Rhoades, R.W. (1992). Differential effects of peripheral damage on vibrissa-related patterns in trigeminal nucleus principalis, subnucleus interpolaris, and subnucleus caudalis. Neuroscience *49*, 141–156.

Cline, H.T., Debski, E.A., and Constantine-Paton, M. (1987). *N*-methyl-D-aspartate receptor antagonist desegregates eye-specific stripes. Proc. Natl. Acad. Sci. USA *84*, 4342–4345.

Dudek, S.M., and Bear, M.F. (1992). Homosynaptic long-term depression in area CA1 of hippocampus and effects of *N*-methyl-D-aspartate receptor blockade. Proc. Natl. Acad. Sci. USA *89*, 4363–4367.

Dudek, S.M., and Bear, M.F. (1993). Bidirectional long-term modification of synaptic effectiveness in the adult and immature hippocampus. J. Neurosci. *13*, 2910–2918.

Erzurumlu, R.S., and Jhaveri, S. (1992). Trigeminal ganglion cell processes are spatially ordered prior to the differentiation of the vibrissa pad. J. Neurosci. *12*, 3946–3955.

Forrest, D., Yuzaki, M., Soares, H.D., Ng, L., Luk, D.C., Sheng, M., Stewart, C.L., Morgan, J.I., Connor, J.A., and Curran, T. (1994). Targeted disruption of NMDA receptor 1 gene abolishes NMDA response and results in neonatal death. Neuron *13*, 325–338.

Goodman, C.S., and Shatz, C.J. (1993). Developmental mechanisms that generate precise patterns of neural connectivity. Cell *72*/Neuron *10* (Suppl.), 77–98.

Harris, K.M., and Teyler, T.J. (1984). Developmental onset of long-term potentiation in area CA1 of the rat hippocampus. J. Physiol. *346*, 27–48.

Hsu, S.-M., Raine, L., and Fanger, H. (1981). Use of avidin-biotin-peroxidase complex (ABC) in immunoperoxidase techniques: a comparison between ABC and unlabeled antibody (PAP) procedures. J. Histochem. Cytochem. *29*, 577–580.

Ikeda, K., Nagasawa, M., Mori, H., Araki, K., Sakimura, K., Watanabe, M., Inoue, Y., and Mishina, M. (1992). Cloning and expression of the ϵ4 subunit of the NMDA receptor channel. FEBS Lett. *313*, 34–38.

Ikeda, K., Araki, K., Takayama, C., Inoue, Y., Yagi, T., Aizawa, S., and Mishina, M. (1995). Reduced spontaneous activity of mice defective in the ϵ4 subunit of the NMDA receptor channel. Mol. Brain Res. *33*, 61–71.

Izumi, Y., and Zorumski, C.F. (1995). Developmental changes in long-term potentiation in CA1 of rat hippocampal slices. Synapse *20*, 19–23.

Kleinschmidt, A., Bear, M.F., and Singer, W. (1987). Blockade of "NMDA" receptors disrupts experience-dependent plasticity of kitten striate cortex. Science *238*, 355–358.

Kutsuwada, T., Kashiwabuchi, N., Mori, H., Sakimura, K., Kushiya, E., Araki, K., Meguro, H., Masaki, H., Kumanishi, T., Arakawa, M., and Mishina, M. (1992). Molecular diversity of the NMDA receptor channel. Nature *358*, 36–41.

Larson, J., Wong, D., and Lynch, G. (1986). Patterned stimulation at the θ frequency is optimal for the induction of hippocampal long-term potentiation. Brain Res. *368*, 347–350.

Li, Y., Erzurumlu, R.S., Chen, C., Jhaveri, S., and Tonegawa, S. (1994). Whisker-related neuronal patterns fail to develop in the trigeminal brainstem nuclei of NMDAR1 knockout mice. Cell *76*, 427–437.

Ma, P.M. (1991). The barrelettes—architectonic vibrissal representations in the brainstem trigeminal complex of the mouse. I. Normal structural organization. J. Comp. Neurol. *309*, 161–199.

MacDermott, A.B., Mayer, M.L., Westbrook, G.L., Smith, S.J., and Barker, J.L. (1986). NMDA-receptor activation increases cytoplasmic calcium concentration in cultured spinal cord neurones. Nature *321*, 519–522.

Malenka, R.C., and Nicoll, R.A. (1993). NMDA-receptor-dependent synaptic plasticity: multiple forms and mechanisms. Trends Neurosci. *16*, 521–527.

Manabe, T., Wyllie, D.J.A., Perkel, D.J., and Nicoll, R.A. (1993). Modulation of synaptic transmission and long-term potentiation: effects on paired pulse facilitation and EPSC variance in the CA1 region of the hippocampus. J. Neurophysiol. *70*, 1451–1459.

Manzoni, O.J., Manabe, T., and Nicoll, R.A. (1994). Release of adenosine by activation of NMDA receptors in the hippocampus. Science *265*, 2098–2101.

Mayer, M.L., Westbrook, G.L., and Guthrie, P.B. (1984). Voltage-dependent block by Mg^{2+} of NMDA responses in spinal cord neurones. Nature *309*, 261–263.

Meguro, H., Mori, H., Araki, K., Kushiya, E., Kutsuwada, T., Yamazaki, M., Kumanishi, T., Arakawa, M., Sakimura, K., and Mishina, M. (1992). Functional characterization of a heteromeric NMDA receptor channel expressed from cloned cDNAs. Nature *357*, 70–74.

Miller, K.D., Chapman, B., and Stryker, M.P. (1989). Visual responses in adult cat visual cortex depend on *N*-methyl-D-aspartate receptors. Proc. Natl. Acad. Sci. USA *86*, 5183–5187.

Mishina, M., Mori, H., Araki, K., Kushiya, E., Meguro, H., Kutsuwada, T., Kashiwabuchi, N., Ikeda, K., Nagasawa, M., Yamazaki, M., et al. (1993). Molecular and functional diversity of the NMDA receptor channel. Ann. NY Acad. Sci. *707*, 136–152.

Monyer, H., Sprengel, R., Schoepfer, R., Herb, A., Higuchi, M., Lomeli, H., Burnashev, N., Sakmann, B., and Seeburg, P.H. (1992). Heteromeric NMDA receptors: molecular and functional distinction of subtypes. Science *256*, 1217–1221.

Monyer, H., Burnashev, N., Laurie, D.J., Sakmann, B., and Seeburg, P.H. (1994). Developmental and regional expression in the rat brain and functional properties of four NMDA receptors. Neuron *12*, 529–540.

Mori, H., and Mishina, M. (1995). Structure and function of the NMDA receptor channel. Neuropharmacology *34*, 1219–1237.

Moriyoshi, K., Masu, M., Ishii, T., Shigemoto, R., Mizuno, N., and Nakanishi, S. (1991). Molecular cloning and characterization of the rat NMDA receptor. Nature *354*, 31–37.

Mulkey, R.M., and Malenka, R.C. (1992). Mechanisms underlying induction of homosynaptic long-term depression in area CA1 of the hippocampus. Neuron *9*, 967–975.

Muller, D., Oliver, M., and Lynch, G. (1989). Developmental changes in synaptic properties in hippocampus of neonatal rats. Dev. Brain Res. *49*, 105–114.

Nowak, L., Bregestovski, P., Ascher, P., Herbet, A., and Prochiantz, A. (1984). Magnesium gates glutamate-activated channels in mouse central neurones. Nature *307*, 462–465.

Perkel, D.J., Hestrin, S., Sah, P., and Nicoll, R.A. (1990). Excitatory synaptic currents in Purkinje cells. Proc. R. Soc. Lond. (B) *241*, 116–121.

Quinlan, J.E., and Davies, J. (1985). Excitatory and inhibitory responses of Purkinje cells, in the rat cerebellum *in vivo*, induced by excitatory amino acids. Neurosci. Lett. *60*, 39–46.

Sakimura, K., Yoshida, Y., Nabeshima, Y., and Takahashi, Y. (1980). Biosynthesis of the brain-specific 14-3-2 protein in a cell-free system from wheat germ extract directed with poly(A)-containing RNA from rat brain. J. Neurochem. *34*, 687–693.

Sakimura, K., Kutsuwada, T., Ito, I., Manabe, T., Takayama, C., Kushiya, E., Yagi, T., Aizawa, S., Inoue, Y., Sugiyama, H., and Mishina, M. (1995). Reduced hippocampal LTP and spatial learning in mice lacking NMDA receptor ε1 subunit. Nature *373*, 151–155.

Schmechel, D., Marangos, P.J., Zis, A.P., Brightman, M., and Goodwin, F.K. (1978). Brain enolases as specific markers of neuronal and glial cells. Science *199*, 313–315.

Seeburg, P.H. (1993). The molecular biology of mammalian glutamate receptor channels. Trends Neurosci. *16*, 359–365.

Shen, H., and Semba, K. (1994). A direct retinal projection to the dorsal raphe nucleus in the rat. Brain Res. *635*, 159–168.

Stefanini, M., De Martino, C., and Zamboni, L. (1967). Fixation of ejaculated spermatozoa for electron microscopy. Nature *216*, 173–174.

Watanabe, M., Inoue, Y., Sakimura, K., and Mishina, M. (1992). Developmental changes in distribution of NMDA receptor channel subunit mRNAs. Neuroreport *3*, 1138–1140.

Watanabe, M., Mishina, M., and Inoue, Y. (1994a). Distinct spatiotemporal expressions of five NMDA receptor channel subunit mRNAs in the cerebellum. J. Comp. Neurol. *343*, 513–519.

Watanabe, M., Mishina, M., and Inoue, Y. (1994b). Distinct gene expression of the *N*-methyl-D-aspartate receptor channel subunit in peripheral neurons of the mouse sensory ganglia and adrenal gland. Neurosci. Lett. *165*, 183–186.

Westneat, M.W., and Hall, W.G. (1992). Ontogeny of feeding motor patterns in infant rat: an electromyographic analysis of suckling and chewing. Behav. Neurosci. *106*, 539–554.

Wong-Riley, M.T.T. (1979). Changes in the visual system of monocularly sutured or enucleated cats demonstrable with cytochrome oxidase histochemistry. Brain Res. *171*, 11–28.

Wong-Riley, M.T.T. (1989). Cytochrome oxidase: an endogenous metabolic marker for neuronal activity. Trends Neurosci. *12*, 94–101.

Wong-Riley, M.T.T., and Welt, C. (1980). Histochemical changes in cytochrome oxidase of cortical barrels after vibrissal removal in neonatal and adult mice. Proc. Natl. Acad. Sci. USA *77*, 2333–2337.

Yagi, T., Nada, S., Watanabe, N., Tamemoto, H., Kohmura, N., Ikawa, Y., and Aizawa, S. (1993a). A novel negative selection for homologous recombinations using diphtheria toxin A fragment gene. Anal. Biochem. *214*, 77–86.

Yagi, T., Tokunaga, T., Furuta, Y., Nada, S., Yoshida, M., Tsukada, T., Saga, Y., Takeda, N., Ikawa, Y., and Aizawa, S. (1993b). A novel ES cell line, TT2, with high germline-differentiating potency. Anal. Biochem. *214*, 70–76.

Yamazaki, M., Mori, H., Araki, K., Mori, K.J., and Mishina, M. (1992). Cloning, expression and modulation of mouse NMDA receptor subunit. FEBS Lett. *300*, 39–45.